catalysts

MDPI

Article

N_2O Decomposition over Cu–Zn/γ–Al_2O_3 Catalysts

Runhu Zhang [1], Chao Hua [2,*], Bingshuai Wang [3] and Yan Jiang [3]

1 Department of Chemical Engineering, Kunming Metallurgy College, Kunming 650033, China; rhzhgyj@gmail.com
2 Key Laboratory of Green Process and Engineering, Institute of Process Engineering, Chinese Academy of Sciences, Beijing 100190, China
3 Liaoning Kelong Fine Chemical Co., Ltd., Liaoyang 111003, China; bingshuai_wang@126.com (B.W.); yan_jiangch@126.com (Y.J.)
* Correspondence: huachao@home.ipe.ac.cn; Tel./Fax: +86-10-8254-4914

Academic Editors: Shaobin Wang and Xiaoguang Duan
Received: 20 November 2016; Accepted: 6 December 2016; Published: 12 December 2016

Abstract: Cu–Zn/γ–Al_2O_3 catalysts were prepared by the impregnation method. Catalytic activity was evaluated for N_2O decomposition in a fixed bed reactor. The fresh and used catalysts were characterized by several techniques such as BET surface area, X-ray diffraction (XRD), and scanning electron microscopy (SEM). The Cu–Zn/γ–Al_2O_3 catalysts exhibit high activity and stability for N_2O decomposition in mixtures simulating real gas from adipic acid production, containing N_2O, O_2, NO, CO_2, and CO. Over the Cu–Zn/γ–Al_2O_3 catalysts, 100% of N_2O conversion was obtained at about 601 °C at a gas hourly space velocity (GHSV) of 7200 h^{-1}. Cu–Zn/γ–Al_2O_3 catalysts also exhibited considerably good durability, and no obvious activity loss was observed in the 100 h stability test. The Cu–Zn/γ–Al_2O_3 catalysts are promising for the abatement of this powerful greenhouse gas in the chemical industry, particularly in adipic acid production.

Keywords: N_2O-decomposition; Cu–Zn/γ–Al_2O_3 catalysts; greenhouse gases; real industrial conditions

1. Introduction

Environmental issues such as global warming and ozone layer depletion are now of universal concern. Nitrous oxide (N_2O) has attracted a great attention as the third most significant anthropogenic greenhouse gas and the largest stratospheric ozone depleting substance [1–5]. N_2O has a lifetime of 114–130 years under atmospheric conditions, and the global warming potential (GWP) of nitrous oxide is about 310 times of carbon dioxide (CO_2) [6]. The emission of N_2O comes from both natural sources and human contributions. Anthropogenic sources, adipic acid production, nitric acid manufacturing, fuel and biomass combustion, and vehicle emissions are considered significant [7]. Therefore, development of efficient technologies for effective N_2O removal has become an emerging issue. A number of methods can potentially be employed to remove N_2O emissions, such as thermal decomposition, selective catalytic reduction with hydrocarbons (HC-SCR), adsorption, and direct catalytic decomposition into O_2 and N_2 [8]. Among various types of abatement technologies, direct catalytic decomposition of N_2O ($N_2O \rightarrow N_2 + 1/2O_2$) is a relatively simple and cost-effective way to remove N_2O from industrial tail gases, and becomes one of the most attracting methods. A large number of catalysts, such as supported noble metals, pure and mixed oxides, and zeolite-based catalysts have been evaluated for N_2O decomposition reaction [9–21]. Among them, noble metal-based catalysts exhibit satisfactory activity at intermediate temperatures [22,23]. However, their high cost represents an important obstacle towards practical applications. Furthermore, their catalytic efficiency is notably hindered by the presence of O_2, NO, and CO, which usually coexist in an exhaust gas stream. Copper-based materials have a great advantage because of their low cost and excellent catalytic performance. However, its thermal stability is not the best, at more than 500 °C. One problem that

still exists in many cases is the deactivation of the catalyst, so it is necessary to replace the catalyst. Therefore, attempts have been made to provide a catalyst for decomposition N_2O, and the catalyst has a thermal stability at high temperature. The study of N_2O catalytic decomposition is mainly focusing on the low temperature catalyst. However, the development of the catalyst should always be consistent with the special characteristics of the pollutant's source, and is not limited by the low temperature catalytic performance [24]. It is an object of the present research to provide a catalyst for N_2O catalytic decomposition, which is thermally stable at elevated temperatures.

The current research study is focused on the abatement of nitrous oxide from adipic acid production facilities. The real conditions of the plant (i.e., in the presence of CO, CO_2, and O_2 and at a high N_2O concentration) are very important to enlighten differences in terms of activity and stability; the latter is a crucial point for the decomposition of a highly concentrated N_2O stream. Thus, the goal of the present work was to test a Cu–Zn/γ–Al_2O_3 catalyst for N_2O decomposition in a model atmosphere from adipic acid production. The catalyst was characterized before and after the catalytic tests in order to identify potential changes in the physico-chemical properties and how these changes could affect the catalyst performance. The stability of Cu–Zn/γ–Al_2O_3 catalysts for long term use in high temperatures was also investigated.

2. Experimental Section

2.1. Catalyst Preparation

The Cu–Zn-based catalysts supported on γ–Al_2O_3 (Changling Catalyst Factory) were prepared via an impregnation method. Before impregnation, γ–Al_2O_3 was calcined at 450 °C for 4 h under an air atmosphere. In a typical impregnation process, $Cu(NO_3)_2{\cdot}3H_2O$ (Sinopharm Chemical Reagent Co., Ltd., Shanghai, China, A.C.S. grade) and $Zn(NO_3)_2{\cdot}6H_2O$ (Sinopharm Chemical Reagent Co., Ltd., Shanghai, China, A.C.S. grade) were dissolved in distilled water with a Cu/Zn molar ratio of 1:7. $Ni(NO_3)_2{\cdot}6H_2O$ (Sinopharm Chemical Reagent Co., Ltd., Shanghai, China, A.C.S. grade) was also added to the distilled water. The amounts of $Ni(NO_3)_2{\cdot}6H_2O$ used for precursors of metal promoter were 3% of CuO and ZnO total mass. A certain amount of γ–Al_2O_3 was added into the solution and kept at ambient temperature for 4 h. Then, excess water was evaporated at 90 °C on a hot plate. The slurry was oven dried at 120 °C for 10 h and calcined in air flow at 800 °C for 4 h. This prepared catalyst was denoted as Cu–Zn/γ–Al_2O_3.

2.2. Catalysts Characterization

BET surface area, pore volume and pore diameter of the catalysts were analyzed by N_2 adsorption at −196 °C using a Micrometrics ASAP 2020 instrument (ASAP2020, Micromeritics, Micromeritics Instrument Corporation, Norcross, GA, USA). XRD patterns of the catalysts were obtained by an X-ray diffractometer (XRD-7000, Shimadzu, Shimadzu Corporation, Kyoto, Japan) in with Cu Kα radiation. The 2θ range was kept between 10 and 80 degrees with a scan speed of $6^\circ{\cdot}min^{-1}$. Measurements of the surface morphology and composition of catalyst were performed using scanning electron microscopy (SEM) with associated energy-dispersive X-ray spectroscopy (EDS) (Quanta 400F, FEI Company, Hillsboro, OR, USA).

2.3. Activity Tests

The catalytic tests in the decomposition of N_2O were performed in a fixed-bed quartz reactor of 10 mm internal diameter containing 0.8 g of catalyst. Two protocols were applied for catalytic evaluation. The reactant gas mixture (12 vol % N_2O, 16.8 vol % O_2, N_2 balance) was fed to the reactor. The total flow rate was 120 $mL{\cdot}min^{-1}$, which could be converted to a gas hourly space velocity (GHSV) of 7200 h^{-1}. The N_2O conversion performance was evaluated in a temperature range of 300–620 °C at a 2 °C/min rate. The composition of outlet gases was analyzed using an on-line gas SP-3420 gas chromatograph (GC) equipped with a thermal conductivity detector (TCD). Figure 1 shows the

schematic of the proposed experimental set-up. The N_2O conversion was determined according to the following equation:

$$X_{N_2O}(\%) = \frac{(C_{N_2O_{in}} - C_{N_2O_{out}})}{C_{N_2O_{in}}} \times 100$$

where X_{N2O} was the percent conversion of N_2O; C_{N2Oin} and C_{N2Oout} were concentrations of N_2O (ppm) in the inlet and outlet, respectively.

The catalytic performance was also evaluated in a gas mixture (12 vol % N_2O, 16.8 vol % O_2, 2.02 vol % CO_2, 696 ppm CO, 134 ppm NO_2, 211 ppm NO, N_2 balance). The composition simulates real waste gas from adipic acid production. A long-term stability test was done at 601 °C where GHSV = 7200 h^{-1}.

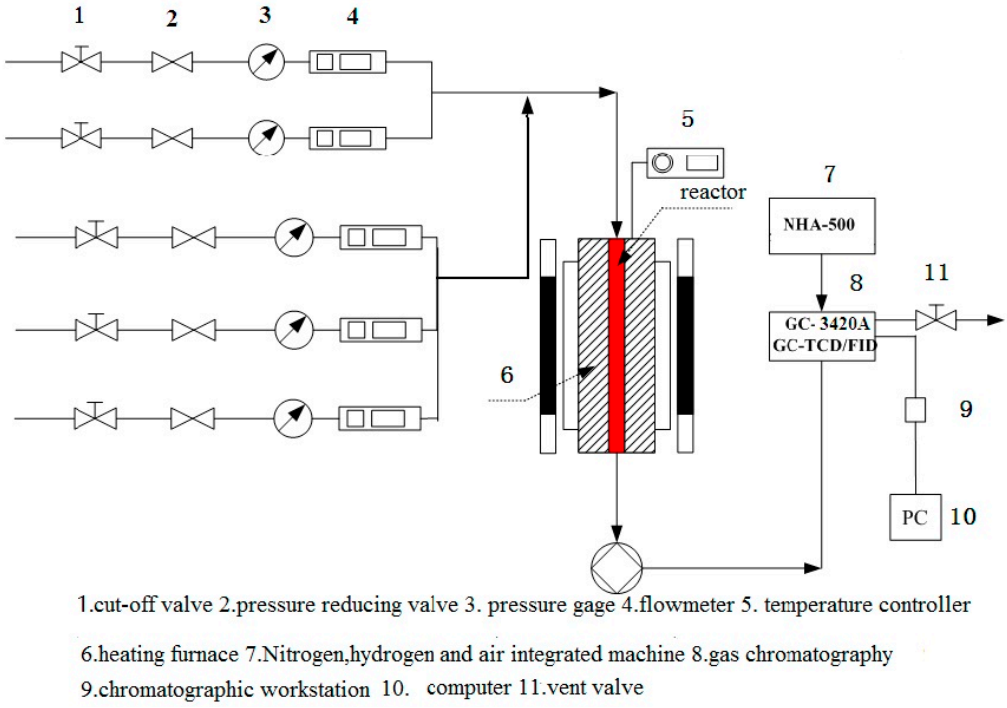

Figure 1. Schematic of the experimental set-up.

3. Results and Discussion

3.1. Effect of Cu–Zn Loading Amount on N_2O Decomposition

In order to investigate the effect of Cu–Zn loading amount for N_2O decomposition, several Cu–Zn/γ–Al_2O_3 catalysts with different Cu–Zn loading amounts were prepared. The feed stream consisted of 7 vol % N_2O, 2 vol % O_2, and balanced N_2. Figure 2 shows the effect of the Cu–Zn loading amount on the decomposition of N_2O as a function of temperature. As shown in Figure 1, below 450 °C, the catalytic activity increased progressively with the increase in Cu–Zn loading amount in the range of 30–45 wt %. Above 450 °C, the catalytic activity increased with the increase in Cu–Zn loading amount, and the catalytic activity then decreased when the Cu–Zn loading amount increased to 45 wt %. The effect of the Cu–Zn loading amount on catalytic activity was more significant above 450 °C. This result may suggest that a suitable Cu–Zn loading amount is 35–40 wt %. The 35 wt % Cu–Zn loading catalyst shows T_{50} (the temperatures of 50% conversion) at 480 °C. Hence, this 35 wt % Cu–Zn loading amount was considered optimum for N_2O decomposition, and further studies were carried out using this catalyst.

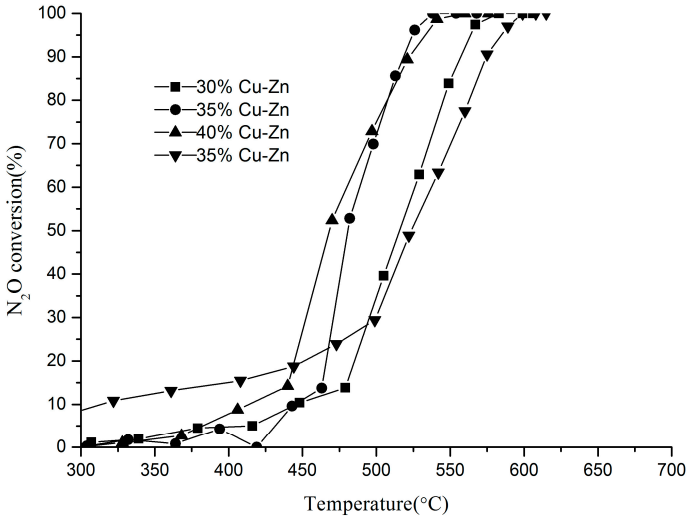

Figure 2. The effect of the Cu–Zn loading amount on the decomposition of N_2O.

3.2. Characterization of the Catalyst

The XRD patterns of the fresh and used Cu–Zn/γ–Al_2O_3 catalysts are shown in Figure 3. In the PDF#44-0706 card of CuO, the characteristic diffraction peaks of 2θ values are at 38.472°, 35.244°, and 48.589°. In the PDF#36-1451 card of ZnO, the characteristic diffraction peaks of 2θ values are at 31.769°, 36.252°, 47.538°, 56.602°, and 66.378° However, for the XRD patterns of Cu–Zn/γ–Al_2O_3, the sharp diffraction peaks were at 2θ = 31.35°, 36.88°, 45.30°, 55.57°, 59.26°, and 65.59°. They were somewhat different from the PDF card of CuO and ZnO. These peaks should be attributed to characteristic diffraction peaks of Cu–Zn composite metal oxides. The detected phase is similar to the spinel phase. The crystal particle sizes of fresh and used catalysts were 6.92 nm and 7.01 nm, respectively. From the XRD spectra, it was found that the diffractograms of the fresh and used catalysts were identical, and no structural changes appeared due to working in real conditions.

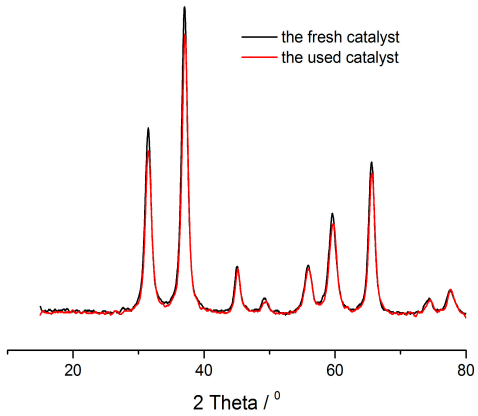

Figure 3. X-ray diffractograms of the fresh catalyst and used catalyst.

The BET textural characteristics of the fresh and used catalyst are reported in Table 1. The surface area of the pure support γ–Al_2O_3 was also measured as 597 m^2/g. Incorporation of Cu–Zn into the alumina support resulted in a slight decrease in surface area. As observed, the surface areas obtained before and after the catalytic tests are not notably changed, indicating that the catalyst has good structural stability. It is also observed that the used catalyst show a lower pore diameter than the fresh catalysts. However, the pore volume is lower in the case of the fresh catalyst compared to the used catalyst. This may be due to the formation of fine pores.

Table 1. Textural characteristics of the fresh and used catalyst.

Catalyst	BET Area ($m^2 \cdot g^{-1}$)	Pore Diameter (nm)	Pore Volume ($cm^3 \cdot g^{-1}$)
fresh	506	6.36	0.8038
used	564	6.10	0.8562
γ–Al_2O_3	597	7.16	1.0704

Figure 4 shows the surface morphology of the fresh and used catalyst. The surface of the catalyst is cabbage shape and very rough. Its microstructure appears a spongy morphology. The components are evenly distributed on the carrier surface. There was no obvious change in the surface morphology of the fresh and used catalyst.

The EDS patterns of the fresh and used catalyst are given in Figure 5. It is observed clearly that the expected elements such as Cu, Zn, and Ni are involved in the surface of the catalyst confirmed by the EDS survey, and the atom ratio of Cu/Zn on the surface before the reaction is 5.36 from the EDS result. Moreover, the atom ratio of Cu/Zn on the surface after the reaction is 5.34, indicating that the content of Cu elements on the catalyst decreased after the reaction. Quantitative EDS analysis of Cu–Zn/γ–Al_2O_3 catalysts are reported in Table 2. EDS analysis shows the content variation of the catalyst components during the reaction. Oxygen and aluminum were lost during the reaction, which led to an increase in Cu, Zn, and Ni.

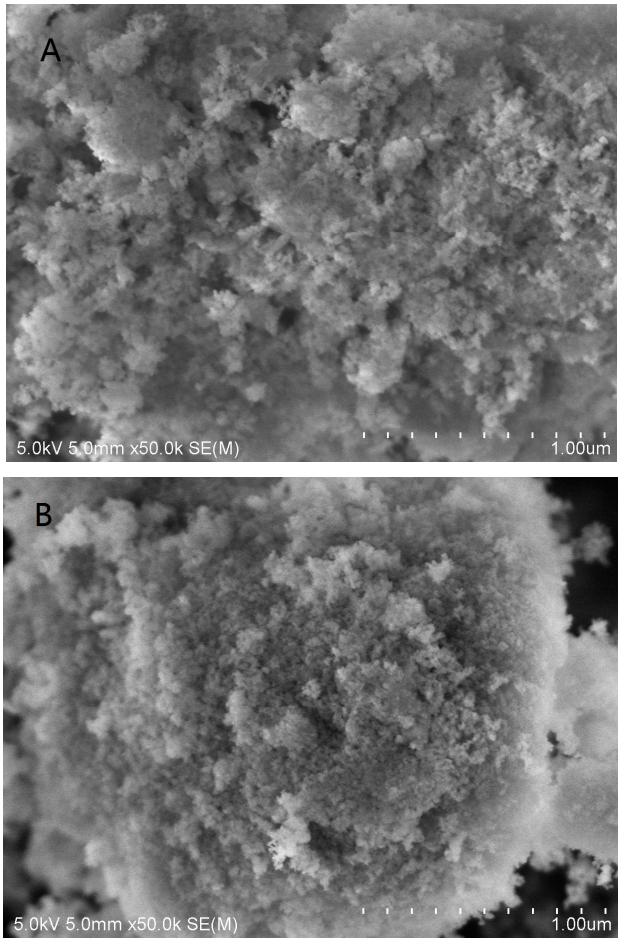

Figure 4. SEM (scanning electron microscope) images of catalysts (**A**) the fresh catalyst and (**B**) the used catalyst.

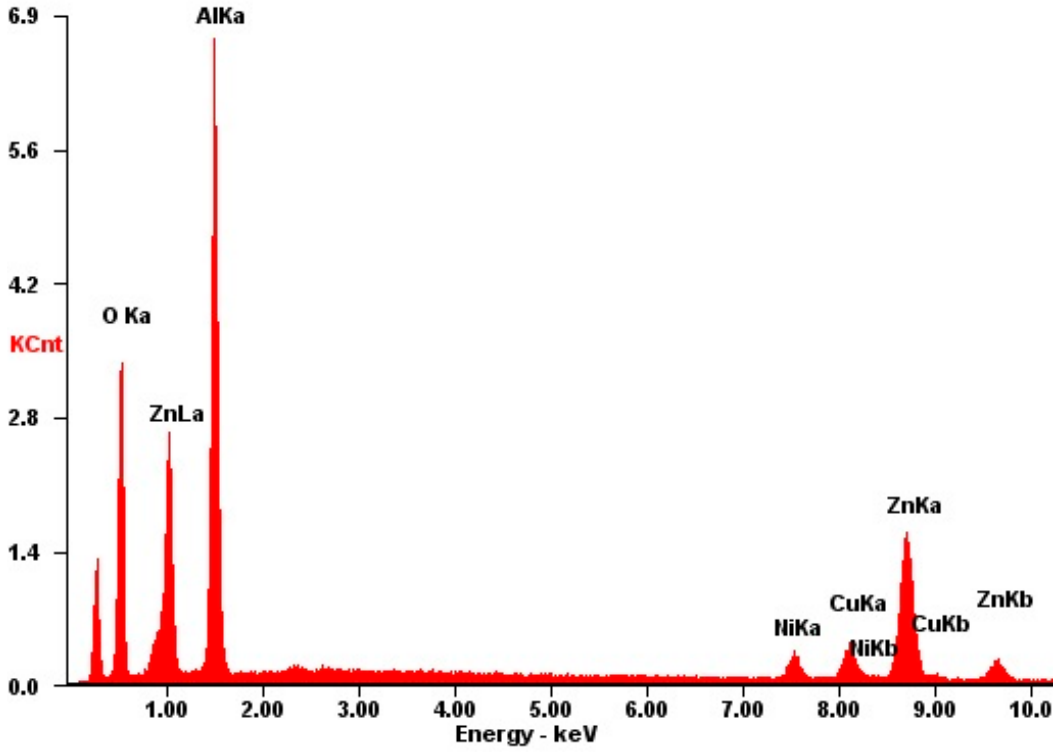

(**A**)

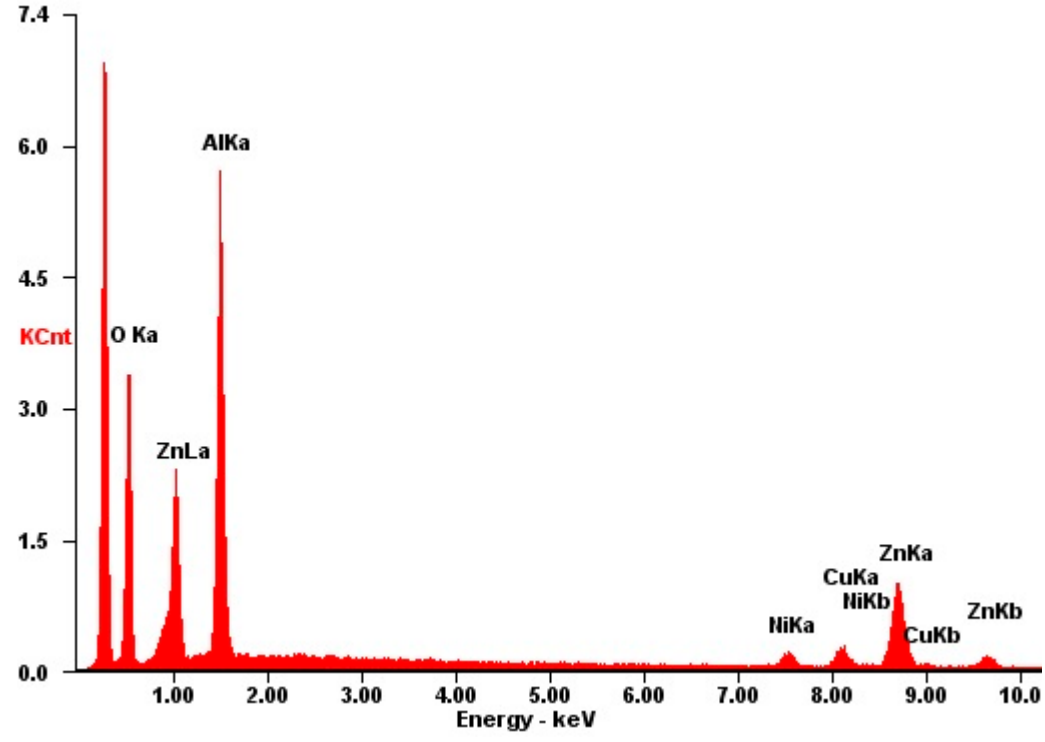

(**B**)

Figure 5. The EDS (energy dispersive spectroscopy)patterns of catalysts (**A**) the fresh catalyst and (**B**) the used catalyst.

Table 2. Quantitative EDS analysis of Cu–Zn/γ–Al_2O_3 catalysts.

Catalyst	wt %				
	O	Al	Ni	Cu	Zn
fresh	24.67	32.61	3.05	6.09	33.58
used	18.85	30.84	3.34	7.23	39.74

3.3. Catalytic Performance

N_2O decomposition studies were carried out on the Cu–Zn/ γ–Al_2O_3 catalysts using Gas Mixture A (12% vol N_2O, 16.8% vol O_2, N_2 balance) and Gas Mixture B (12% vol N_2O, 16.8% vol O_2, 2.02% vol CO_2, 696 ppm CO, 134 ppm NO_2, 211 ppm NO, N_2 balance). The catalyst with 35 wt % Cu/Zn was used, unless otherwise stated. As shown in Figure 6, Cu–Zn/γ–Al_2O_3 catalysts are virtually not active below 400 °C, and they start to show some activities above 425 °C. Compared with Gas Mixture A, Gas Mixture B has more components, but the reaction temperature is lower, which is related to the reduction of CO and NO in Gas Mixture B. When N_2O was totally converted (more than 99%), the reaction temperature of Gas Mixture B was 561 °C, which is 42 °C lower than Gas Mixture A. After the catalytic reaction, the main components of the mixed gas were O_2 and N_2, so the catalyst could effectively eliminate N_2O. The temperatures of 50% conversion (T_{50}) were read out from the curves and are listed in Table 3.

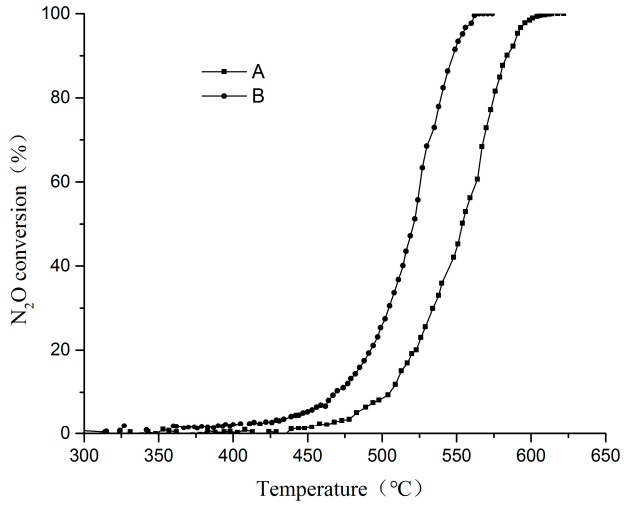

Figure 6. Conversion of N_2O over Cu–Zn/γ–Al_2O_3 catalysts. Reaction conditions: (A) 12% vol N_2O, 16.8% vol O_2, N_2 balance; GHSV (gas hourly space velocity) = 7200 h^{-1}; (B) 12% vol N_2O, 16.8% vol O_2, 2.02% vol CO_2, 696 ppm CO, 134 ppm NO_2, 211 ppm NO; N_2 balance; GHSV = 7200 h^{-1}.

Table 3. Temperatures of 10%, 50%, and 99% conversion of N_2O (T_{10}, T_{50}, and T_{99}) over the Cu–Zn/γ–Al_2O_3 catalyst.

Gas Mixture A (°C)			Gas Mixture B (°C)		
T_{10}	T_{50}	T_{99}	T_{10}	T_{50}	T_{99}
505	553	603	470	521	561

Measuring the durability of catalysts is important in determining their practical feasibility. Figure 7 shows the catalytic stability of the Cu–Zn/γ–Al_2O_3 catalyst for N_2O decomposition. These tests were carried out at T = 601 °C. In the model atmosphere (Gas Mixture A and Gas Mixture B), N_2O conversion over the Cu–Zn/γ–Al_2O_3 catalyst after reaction at T = 601 °C for 100 h was maintained at 99%, indicating that the catalyst has high activity and stability.

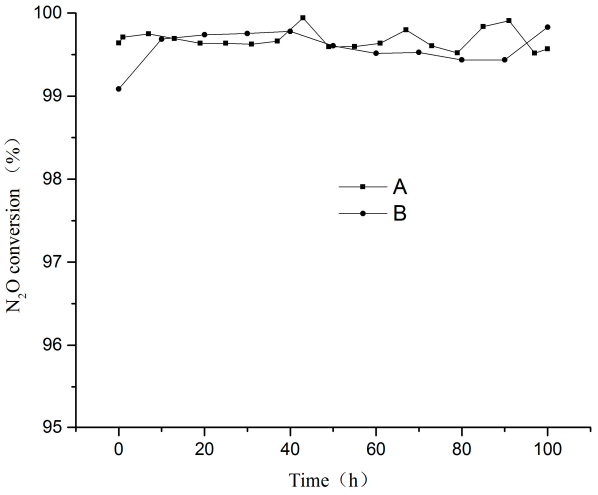

Figure 7. Stability test run of the Cu–Zn/γ–Al_2O_3 catalysts at 601 °C for 100 h.

4. Conclusions

In this study, Cu–Zn/γ–Al_2O_3 catalysts were prepared by an impregnation method and characterized by means of SEM, XRD, and N_2 adsorption–desorption techniques. Prepared catalysts were tested for N_2O catalytic decomposition. The results illustrate that the Cu–Zn/γ–Al_2O_3 catalyst is quite effective for the catalytic decomposition of N_2O under model atmosphere. N_2O can be completely decomposed at 601 °C in oxygen atmosphere. In addition, the Cu–Zn/Al_2O_3 catalyst exhibited appreciable activity even in the presence of CO and NO_2, which are commonly found in exhaust gases from adipic acid production. Good performance and no deactivation of the catalyst were confirmed by 100 h stability tests. This study serves only as an exploratory work on this catalyst system; detailed fundamental studies are underway.

Acknowledgments: The authors gratefully acknowledge the financial support of the National High Technology Research and Development Program of China (2013AA030705).

Author Contributions: Runhu Zhang and Chao Hua conceived and designed the experiments; Runhu Zhang performed the experiments; Bingshuai Wang and Chao Hua analyzed the data; Yan Jiang contributed reagents/materials/analysis tools; Runhu Zhang wrote the paper.

Conflicts of Interest: The authors declare no conflicts of interest.

References

1. Strokal, M.; Kroeze, C. Nitrous oxide (N_2O) emissions from human waste in 1970–2050. *Cur. Opin. Environ. Sustain.* **2014**, *9–10*, 108–121. [CrossRef]
2. Erisman, J.W.; Galloway, J.; Seitzinger, S.; Bleeker, A.; Butterbach–Bahl, K. Reactive nitrogen in the environment and its effect on climate change. *Cur. Opin. Environ. Sustain.* **2011**, *3*, 281–290. [CrossRef]
3. Hungate, B.A.; Dukes, J.S.; Shaw, M.R.; Luo, Y.; Field, C.B. Nitrogen and Climate Change. *Science* **2003**, *302*, 1512–1513. [CrossRef] [PubMed]
4. Davidson, E.A.; Kanter, D. Inventories and scenarios of nitrous oxide emissions. *Environ. Res. Lett.* **2014**, *9*, 105012–105024. [CrossRef]
5. Li, L.; Xu, J.; Hu, J.; Han, J. Reducing Nitrous Oxide Emissions to Mitigate Climate Change and Protect the Ozone Layer. *Environ. Sci. Technol.* **2014**, *48*, 5290–5297. [CrossRef] [PubMed]
6. Zamudio, M.A.; Bensaid, S.; Fino, D.; Russo, N. Influence of the $MgCo_2O_4$ Preparation Method on N_2O Catalytic Decomposition. *Ind. Eng. Chem. Res.* **2011**, *50*, 2622–2627. [CrossRef]
7. Bueno-López, A.; Such-Basáñez, I.; Salinas-Martínez de Lecea, C. Stabilization of active Rh_2O_3 species for catalytic decomposition of N_2O on La-, Pr-doped CeO_2. *J. Catal.* **2006**, *244*, 102–112. [CrossRef]

8. Kumar, S.; Vinu, A.; Subrt, J.; Bakardjieva, S.; Rayalu, S.; Teraoka, Y.; Labhsetwar, N. Catalytic N_2O decomposition on $Pr_{0.8}Ba_{0.2}MnO_3$ type perovskite catalyst for industrial emission control. *Catal. Today* **2012**, *198*, 125–132. [CrossRef]
9. Russo, N.; Fino, D.; Saracco, G.; Specchia, V. N_2O decomposition over various spinel-type oxides. *Catal. Today* **2007**, *119*, 228–232. [CrossRef]
10. Haber, J.; Nattich, M.; Machej, T. Alkali-metal promoted rhodium-on-alumina catalysts for nitrous oxide decomposition. *Appl. Catal. B Environ.* **2008**, *77*, 278–283. [CrossRef]
11. Shen, Q.; Li, L.; Li, J.; Tian, H.; Hao, Z. A study on N_2O catalytic decomposition over Co/MgO catalysts. *J. Hazard. Mater.* **2009**, *163*, 1332–1337. [CrossRef] [PubMed]
12. Wang, Y.; Zhang, J.; Zhu, J.; Yin, J.; Wang, H. Experimental research on catalytic decomposition of nitrous oxide on supported catalysts. *Energy Convers. Manag.* **2009**, *50*, 1304–1307. [CrossRef]
13. Abu-Zied, B.M.; Schiwieger, W.; Unger, A. Nitrous oxide decomposition over transition metal exchanged ZSM-5 zeolites prepared by the solid state ion-exchanged method. *Appl. Catal. B* **2008**, *84*, 277–288. [CrossRef]
14. Pekridis, G.; Kaklidis, N.; Konsolakis, M.; Iliopoulou, E.F.; Yentekakis, I.V.; Marnellos, G.E. Correlation of surface characteristics with catalytic performance of potassium promoted Pd/Al_2O_3 catalysts: The case of N_2O reduction by alkanes or alkenes. *Top. Catal.* **2011**, *54*, 1135–1142. [CrossRef]
15. Russo, N.; Mescia, D.; Fino, D.; Saracco, G.; Specchia, V. N_2O decomposition over perovskite catalysts. *Ind. Eng. Chem. Res.* **2007**, *46*, 4226–4231. [CrossRef]
16. Xue, L.; Zhang, C.; He, H.; Teraoka, Y. Catalytic decomposition of N_2O over CeO_2 promoted Co_3O_4 spinel catalyst. *Appl. Catal. B Environ.* **2007**, *75*, 167–174. [CrossRef]
17. Pasha, N.; Lingaiah, N.; Reddy, P.S.S.; Prasad, P.S.S. An investigation into the effect of Cs promotion on the catalytic activity of NiO in the direct decomposition of N_2O. *Catal. Lett.* **2007**, *118*, 64–68. [CrossRef]
18. Iwanek, E.; Krawczyk, K.; Petryk, J.; Sobczak, J.W.; Kaszkur, Z. Direct nitrous oxide decomposition with CoOx-CeO_2 catalysts. *Appl. Catal. B* **2011**, *106*, 416–422. [CrossRef]
19. Zabilskiy, M.; Djinovic, P.; Tchernychova, E.; Tkachenko, O.P.; Kustov, L.M.; Pintar, A. Nanoshaped CuO/CeO_2 Materials: Effect of the Exposed Ceria Surfaces on Catalytic Activity in N_2O Decomposition Reaction. *ACS Catal.* **2015**, *5*, 5357–5365. [CrossRef]
20. Pacultova, K.; Karaskova, K.; Strakosova, J.; Jiratova, K.; Obalova, L. Supported Co–Mn–Al mixed oxides as catalysts for N_2O decomposition. *C. R. Chim.* **2015**, *18*, 1114–1122. [CrossRef]
21. Pasha, N.; Lingaiah, N.; Reddy, P.S.S.; Prasad, P.S.S. Direct decomposition of N_2O over cesium-doped CuO catalysts. *Catal. Lett.* **2009**, *127*, 101–106. [CrossRef]
22. Konsolakisa, M.; Yentekakisa, I.V.; Pekridisb, G.; Kaklidisb, N.; Psarrasc, A.C.; Marnellosb, G.E. Insights into the role of SO_2 and H_2O on the surface characteristics and de-N_2O efficiency of Pd/Al_2O_3 catalysts during N_2O decomposition in the presence of CH_4 and O_2 excess. *Appl. Catal. B Environ.* **2013**, *138–139*, 191–198. [CrossRef]
23. Kapteijn, F.; Rodriquez-Mirasol, J.; Moulijn, J.A. Heterogeneous catalytic decomposition of nitrous oxide. *Appl. Catal. B Environ.* **1996**, *9*, 25–64. [CrossRef]
24. Konsolakis, M. Recent Advances on Nitrous Oxide (N_2O) Decomposition over Non-Noble-Metal Oxide Catalysts: Catalytic Performance, Mechanistic Considerations, and Surface Chemistry Aspects. *ACS Catal.* **2015**, *5*, 6397–6421. [CrossRef]